PHILOSOPHICAL TRANSACTIONS OF THE ROYAL SOCIETY B BIOLOGICAL SCIENCES

Use of Zone Correction Plates and Other Techniques for Structure Determination of Aperiodic Objects at Atomic Resolution Using a Conventional Electron Microscope

W. Hoppe

Phil. Trans. R. Soc. Lond. B 1971 **261**, 71-94
doi: 10.1098/rstb.1971.0038

Phil. Trans. Roy. Soc. Lond. B. **261**, 71–94 (1971) [71]
Printed in Great Britain

Use of zone correction plates and other techniques for structure determination of aperiodic objects at atomic resolution using a conventional electron microscope

By W. Hoppe
Max Planck Institut für Eiweiss und Lederforschung Munich, Germany

Electron microscopy using microscopes with conventional magnetic lenses is restricted in resolution by spherical aberration. The 'zonal correction principle' allows this limit to be overcome. Its use in image reconstruction schemes allows separation of the influence of defocusing, astigmatism, etc., from the physically significant structure. The use of three-dimensional methods of image differencing is necessary in order to get interpretable results in the study of the not 'infinitely thin' objects in electron microscopy at atomic level.

The use of redundancy principles (similar to X-ray structure determination) is discussed and demonstrated.

The most severe difficulty, especially in electron microscopy of organic specimens, is radiation damage.

Introduction

Some years ago—in fact stimulated by the idea of the zone correction plates for the enhancement of the resolving power of electron lenses (Hoppe 1961)—we became interested in the problem of 'electron microscopy at atomic resolution'. The course of this work soon made it clear that resolution is not the only problem, perhaps not even the most difficult problem. My paper will give a summary of our work; a more detailed account will be found elsewhere (Hoppe 1970*b*). The paper will not cover our work on electron diffraction in a generalized primary beam field (Hoppe 1969*a*); but it should be mentioned that that work is to some extent related to the work reported here, as the problem to be solved is again structure analysis at atomic resolution with electrons.

Periodicity and radiation damage

Let us first start with a not very encouraging discussion concerning the physical possibility of 'molecular microscopy'. It is the strong interaction of electrons with atoms that makes it possible to collect in a reasonable time enough scattered electrons for the recognition of single atoms. But there is also the unhappy situation that for light atoms the cross-sections for elastic and inelastic scattering are of the same order of magnitude (Lenz 1954†). This means that the number of elastic and inelastic collisions is approximately the same. In crystal structure analysis there are many equivalent molecules—in a small protein crystal, for example, there are about 10^{17}! It is therefore highly improbable that a molecule will be hit more than once by an incident quantum. Therefore the elastically scattered quanta will find untouched molecules and can build up diffraction patterns of the non-distorted molecule. Only in cases where a primary radiation reaction is followed by many secondary chemical reactions (as in X-ray crystallography of wet crystals) might radiation damage be a difficulty. It is the *spatial* periodicity which

† It is interesting to note that for X-rays this relation is much worse. Electron scattering is therefore a comparatively weak tool of destruction!

makes crystal structure analysis possible. In the case of an aperiodic object the situation is entirely different. The electrons necessary to represent an atom in the structure must be collected by repetitive scattering from that single atom. It is obvious that a recognition of the atom will only be possible if every elastically scattered electron finds the atom in the same site (but not necessarily in the same chemical state). Inelastic collisions can take place with the nuclei or with the shell electrons. For collisions with nuclei the maximal transferred kinetic energy depends on the accelerating voltage and on the atomic mass. An incident 100 kV electron can, for example, transfer to a hydrogen atom 200 eV, to a carbon atom 20 eV and to a gold atom only 1 eV. If this energy exceeds the bonding energy, a displacement of the atom to another site will take place. If one very roughly estimates this energy threshold to be 5 to 20 eV, one can see that displacements of hydrogen atoms are highly probable, whereas displacements of carbon atoms might occur already at medium accelerating voltages. Heavy atoms will only be knocked out if very high accelerating potentials are used. The displacement of an atom due to the transmitted kinetic energy is a very serious damage. In most cases it will inevitably end the collection of scattered electrons from that atom.

A much broader spectrum of possibilities will occur if one discusses the influence of the incident electrons on the electronic structure of the object studied. Isolated excitations, collective excitations (plasma excitations, phonon excitations), and ionizations will be observed. Let us now remember that inelastic collisons are as frequent as elastic collisions. This relation does not vary appreciably with the accelerating potential contrary to the relative number of atoms ejected by the transmitted kinetic energy of the incident electrons. Therefore a change of the voltage cannot exclude these effects. The situation would be hopeless if a change of the electronic structure in a solid inevitably meant a displacement of atoms. It is the only hope for structure determination of aperiodic objects at atomic resolution that the rearrangement of bonds—and consequently of atoms—is a secondary effect. In principle two schemes can be discussed which could allow the necessary repetitive scattering, (1) conservation and (2) restoration. A conservative mechanism would be 'flash electron microscopy' (Breedlove & Trammell 1970). If in the period between excitation and rearrangement of bonds the scattering experiment could be done, the image would reveal the unchanged structure. Depending on assumptions this time might vary between 10^{-8} s (Schulte-Frohlinde 1970) (life time of a singlet state) and 10^{-13} s (molecular vibration time). Apart from the serious experimental difficulties, space charge effects (Boersch effect) might occur due to the necessary intensity density of the electron beam.

Another proposal is to work at liquid–helium temperatures. Experiments have shown (Siegel 1969) that in fact radiation damage will be substantially reduced. In this case a combination between conservation and restoration might take place: The low mobility of radicals and other fragments (conservation mechanism) might, on the other hand, increase the chance of their recombination (restoration mechanism). Very little radiation damage will occur if mostly plasma waves are excited (as in metals and graphite, but also to some extent in insulators). In this case the energy can be dissipated. Schulte-Frohlinde (1970 and personal communication) has made the interesting proposal of introducing heavy atoms as electron-donors into an organic object (using an appropriate staining process). 'Restoration' in this case will mean replacement of the electrons lost in ionizing events. Thus 'staining' could get a new sense in electron structure determination at atomic resolution. It might facilitate the preservation of the organic structure.

PHILOSOPHICAL TRANSACTIONS OF THE ROYAL SOCIETY B BIOLOGICAL SCIENCES

The hydrogen nuclei ejected by the incident electrons can cause serious difficulty. There is the hope that at very low temperature the life time of the hydrogen-free radicals will be long enough to permit the structural study of the core (under the assumption naturally that the radical structure will not differ significantly from the original structure). One could think also of reactions with hydrogen or hydrating gases (taking place at low pressure in the electron microscope itself) in order to replace the hydrogen (restoration).

Let us summarize: for some types of aperiodic objects there might be a good chance of getting the individual structure; unhappily this prediction is too optimistic for biological molecules. Nobody can say whether we will ever see a protein molecule with the same clarity as in a protein crystal structure analysis. Under the present imaging conditions biological

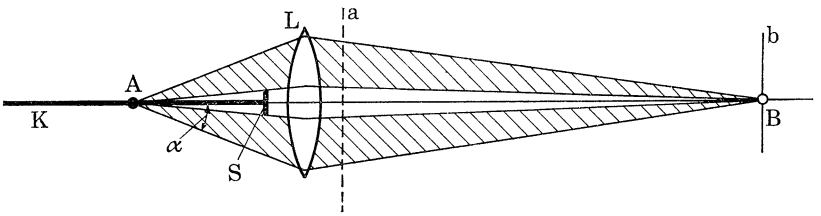

FIGURE 1. Imaging of a single atom A with an ideal lens L. The illuminating plane wave K is screened off behind the atom by a small stop S. So a dark-field image B with coherent illumination of the atom is formed in the Gaussian image plan b; the Fourier transform of the atom appears in the apertive plan a of the lens.

macromolecules probably will be converted to carbon skeletons before a micrograph can be taken. But even a study of these skeletons might perhaps be fruitful for a better understanding of the macromolecules, especially if the 'radiation chemistry' of the reactions becomes clearer.

THE PRINCIPLE OF ZONAL CORRECTION FOR EXTENDING RESOLUTION

Let us consider the most simple example of an electron microscope image: the image of a single atom. The atom A (figure 1) will be illuminated by the monochromatic plane wave K of the wavelength λ (coherent illumination); the primary wave will be screened off by the stop S (coherent dark field illumination). (It might be mentioned, that this scheme is exactly equivalent to the illumination scheme in crystal structure analysis.) We assume an ideal lens L; the image B of the atom will appear in the Gaussian plane b. The maximal scattering angle α sets the resolution limit; we assume a resolution somewhat below the atomic distances (0.1 nm as order of magnitude). In the aperture plane of L the Fourier transform of the atom A will appear, seen with electrons of the wavelength λ. The Fourier amplitude is given by the atomic scattering factor; if we assume for simplicity a point atom with unit scattering power, the amplitude is constant and equal to 1 for all scattering angles. The important point is, that for imaging in the Gaussian plane the phase is also constant for all Fourier coefficients. Therefore at the image point all waves add up to the maximal value without destructive interference. The situation will change, if one replaces the hypothetical ideal electron lens by a conventional magnetic lens with rotational symmetry. These lenses have a high spherical aberration with constants between $C_s \sim 4$ mm and $C_s \sim 1$ mm. (The one-field condenser objective of the Ruska–Riecke type (Ruska 1965) has $C_s = 0.5$ mm.) If one sets again the limit of atomic resolution, one will never get a constant phase in the whole region; the phase γ (= wave aberration) will oscillate several times between 0 and 2π. The number of oscillations depends on the range in

Fourier space, on the coefficient of spherical aberration and on the defocusing parameter. For a certain image plane something like an optimized phase function (criterion: minimal number of oscillations) can be found. Figure 2 shows the real part and the imaginary part of such a pupil function ($P = e^{i\gamma}$) to a resolution of $\sim$ 0.1 nm, calculated for an objective with $C_s = 1$ mm and for 100 kV electrons. It is easy to understand that not very much intensity will be found at the centre of the image point. Following the principles of Fourier transformation one has simply to integrate the functions in figure 2 along the θ-axis and to add the two squared integrals in order to get the dark field intensity in the centre of the image point. One can immediately see, that both integrals must be small, as the positive and the negative regions in figure 2 tend to

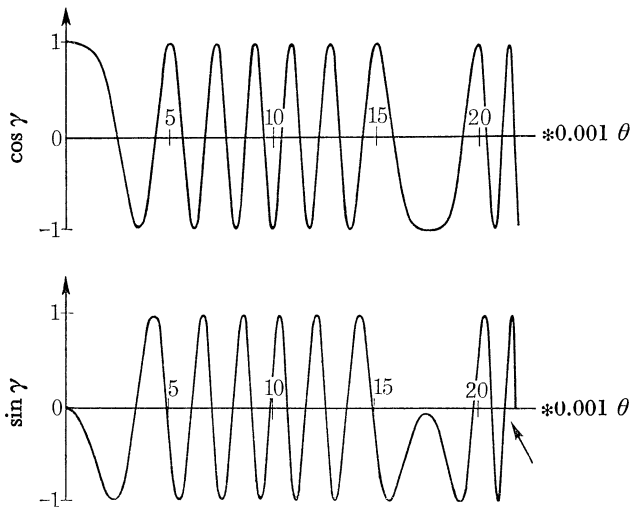

FIGURE 2. Real ($\cos\gamma$) and imaginary part ($\sin\gamma$) of the pupil function $P = \exp(i\gamma)$ with the wave aberration $\gamma = 2\pi/\lambda\ (\frac{1}{4}C_s\theta^4 - \frac{1}{2}z_0\theta^2)$.

U, accelerating voltage of the electrons (100 kV); λ, wavelength of the electrons (3.7 pm (100 kV); for $U = 100$ kV); C_s, constant of spherical aberration (1 mm); z_0, defocusing parameter (310 nm); θ, angle between the direction of the scattered electron and the optical axis; $d = 0.77\lambda/\alpha = 0.13$ nm; is the resolution limit if $\alpha = 0.022$ is the aperture of the objective.

cancel each other. (In the case of the ideal lens the pupil function is simply given by $\cos\gamma = 1$ and $\sin\gamma = 0$; the integral over $\cos\gamma$ has its maximal possible value.) One way to get a higher intensity into the image point is to screen off regions of negative sign in the Fourier transform of the point scatterer. This can be done experimentally, since the transform is produced in the aperture plane of the objective. (In principle the limiting aperture in a conventional electron microscope has the same effect: It screens off the 'wrong' regions in the pupil function (but also correct regions).) It is necessary to incorporate a system of annularly shaped screens into the objective (for an example see figure 3). Figure 4 demonstrates the principle and shows at the same time, that only either for $\cos\gamma$ or for $\sin\gamma$ can the destructive influence of the scattered waves with opposite phases be removed. This has the undesired effect that the amplitude in the centre of the image point will be reduced to about one quarter of the amplitude produced by an ideal lens with the same aperture. (If one replaces the screens by phase shifting foils, the amplitude can be enlarged by a factor of 2 or even 4 (see, for example, Hoppe 1970*a*); calculations (Reimer 1970) have shown, that the gain in contrast surpasses the loss due to the fog.) On the other hand, calculations have shown that the 'image point' character of the ideal lens will be retained. The well-known criterion of the minimal distance between two image points

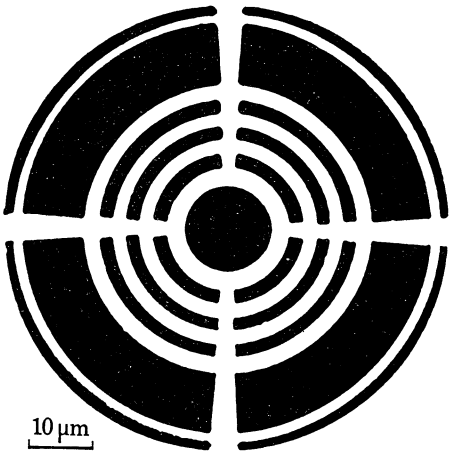

FIGURE 3. Zone plate in the aperture plane of the objective of the Siemens Elmiskop Ia for imaging of weak phase objects in coherent bright-field illumination. Scattered electrons hitting the white regions are screened off. The zone plate is calculated for a wavelength of the electrons $\lambda = 3.7$ pm, (100 keV), a spherical aberration $C_s = 4.1$ mm and a defocusing parameter $z_0 = 522$ nm. The aperture is $\alpha = 0.0142$ rad, the resolution limit $d = 0.77\ \lambda/\alpha = 0.2$ nm.

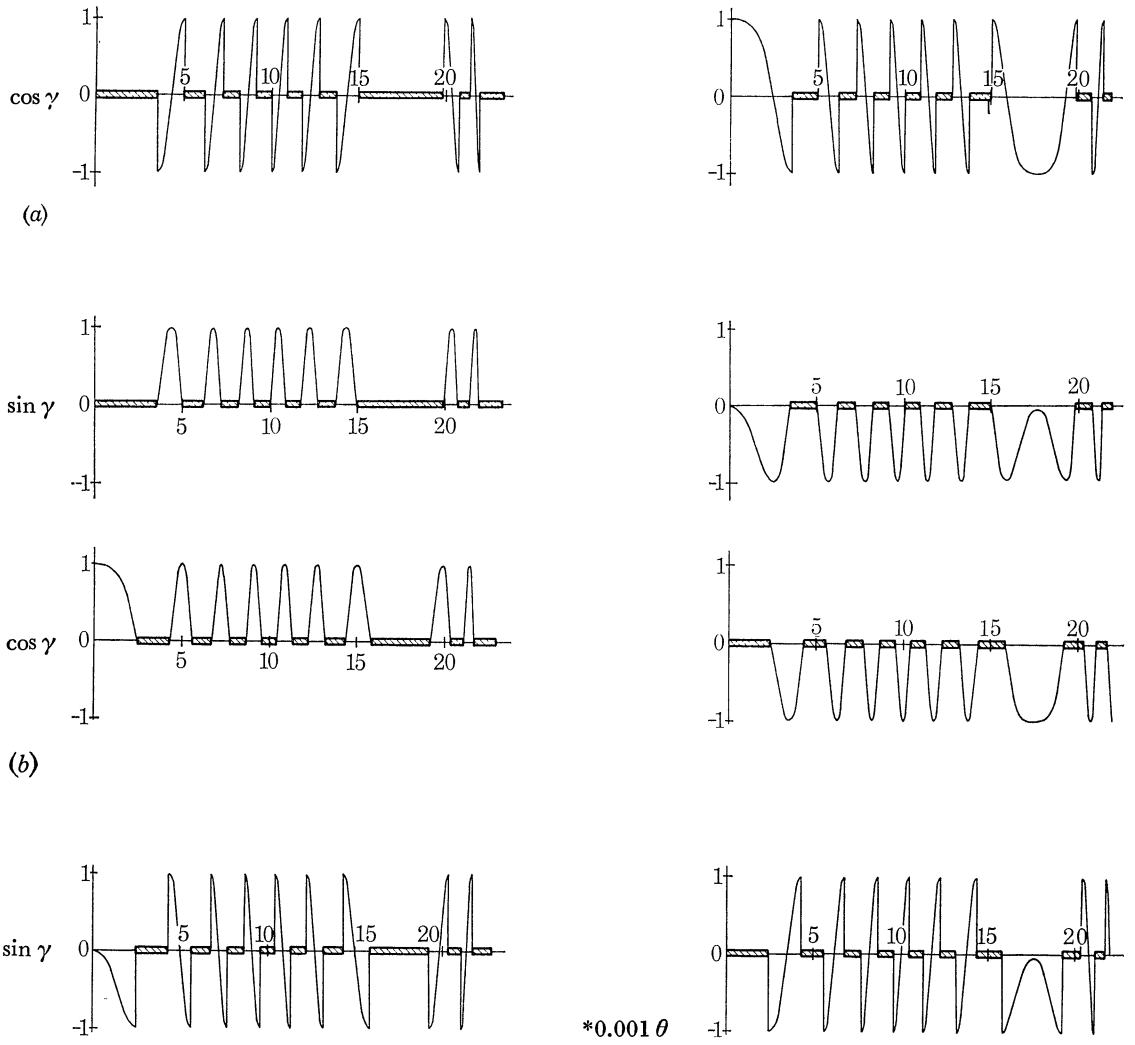

FIGURE 4. Real and imaginary part of the pupil function of figure 2, screened off partly by four types of zone plates. In coherent dark-field illumination all four types can be used for the imaging of weak phase objects or amplitude objects. In coherent bright-field illumination the pupil functions of figure 4*a* are suitable for weak phase objects (on the left for positive, on the right for negative phase contrast), whereas the functions of figure 4*b* are for amplitude objects (on the left for positive, on the right for negative contrast).

can be applied; it leads to the same value as for an ideal lens. If one goes from dark-field illumination to bright-field illumination, one has to add the primary wave. As atoms act approximately as elastic scatterers, the phase shift $\frac{1}{2}\pi$ has to be taken into account; one gets a phase contrast image of the atom (for details of these calculations see Langer & Hoppe 1966/7). This is what could be called the first use of the resolution extending principle of zonal correction in electron microscopy. We know today that there are other ways to correct for the zonal phase oscillations in the pupil function. In retrospect the most important point in this work might be (this became clear) that structure determinations at atomic resolution are in principle possible with conventional electron optics; one does not have to wait until new complicated lens systems with greatly reduced lens errors are developed. The result is not trivial. It is quite a coincidence that at 'atomic resolution' the number of zonal oscillations is of an acceptable order of magnitude. Too rapid oscillations would mean that practical corrections are impossible. A related device to a zone correction plate is a Fresnel lens; it is simply a zone plate, where the lens has been omitted. But the corresponding pupil function has instead of eight oscillations (figure 2) $\sim 10^5$ oscillations! Another way to extend the electron microscope resolution by zonal correction is related to the 'real part' image reconstruction in light optics (Elias, Grey & Robinson 1952). Gabor's proposal of holography with electrons (Gabor 1949) was based on (1) (in the diffraction plane!). This 'linear transfer of amplitudes' is generally important in light optics with coherent sources. If one studies the electron microscope bright field image under the experimental conditions discussed above, the intensity I in the image plane is proportional to

$$I \sim A^2 + A(\psi + \psi^*) + \psi\psi^*. \qquad (1)$$

If A—the amplitude of the primary wave—is much stronger than the image amplitude ψ, then the third term in (1) can be neglected and the modulation of the intensity will be proportional to the real part of the image amplitude ψ. In fact, with very thin objects, the linear approximation for (1) might be too good—the contrast is then extremely low and difficult to measure. We have therefore proposed enhancing the contrast by partial removal of the primary beam (Hoppe 1963; Langer & Hoppe 1966/7); neglect of the third term can be taken into account by calculation. A Fourier transformation reveals therefore the Fourier coefficients of the real part distorted by the pupil function. It is now only necessary to correct the Fourier coefficients corresponding to the pupil function and to reconstruct the undistorted image by a second Fourier transformation. The Fourier operations can be done by calculation or in a laser–optical analogue device. In particular the Fourier transform of the distorted image of a single atom resembles the imaginary part† of the pupil function (see figure 2); thus an excellent means for studying the pupil function would be given. Naturally it is impossible to photograph the image of a single atom; but the over-all Fourier transform of an object, consisting of randomly distributed atoms is very similar to the transform of a single atom. In approximation a supporting film of carbon is such an object. The first experiments (using a light diffractometer) were carried out by Thon in our laboratory,‡ followed by a careful study in the Siemens

† Corresponding to the additional phase shift $\frac{1}{2}\pi$ caused by the elastic scattering on atoms (phase object). An amplitude object (no phase shift) would deliver the real part.

‡ This work had interesting precursors: It was well known, to the electron-microscopists, that supporting films show different granularities in micrographs depending on defocusing. Lenz & Scheffels (1958) have given the correct explanation. Thon (1965) added the spherical aberration into the Lenz theory and started with a statistical survey of point distances in these micrographs. Our first proposal was to use the autocorrelation function for the further study; but it became immediately clear that the use of the Fourier transform is more straightforward.

PHILOSOPHICAL TRANSACTIONS OF THE ROYAL SOCIETY B BIOLOGICAL SCIENCES

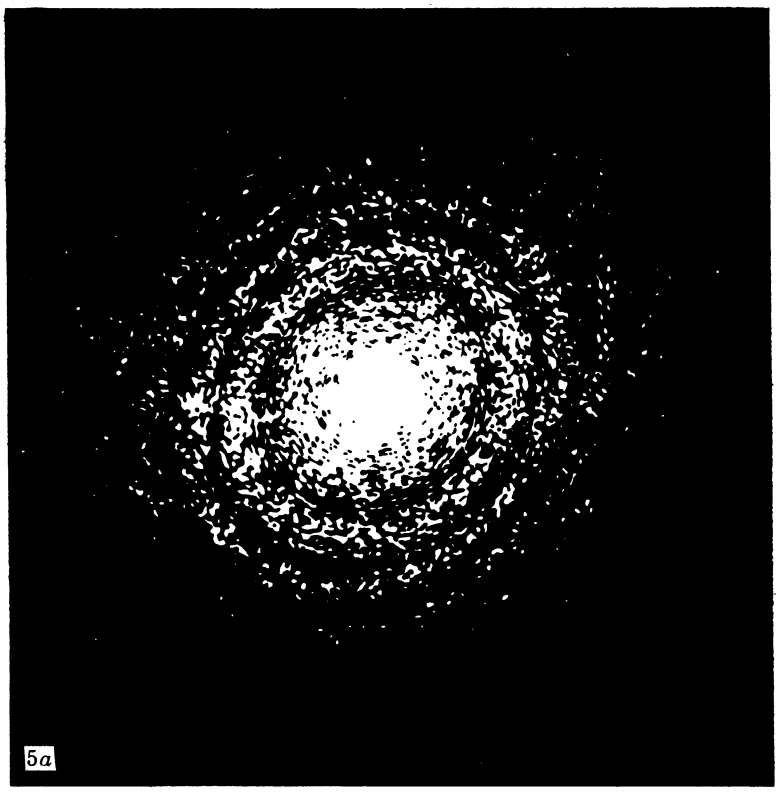

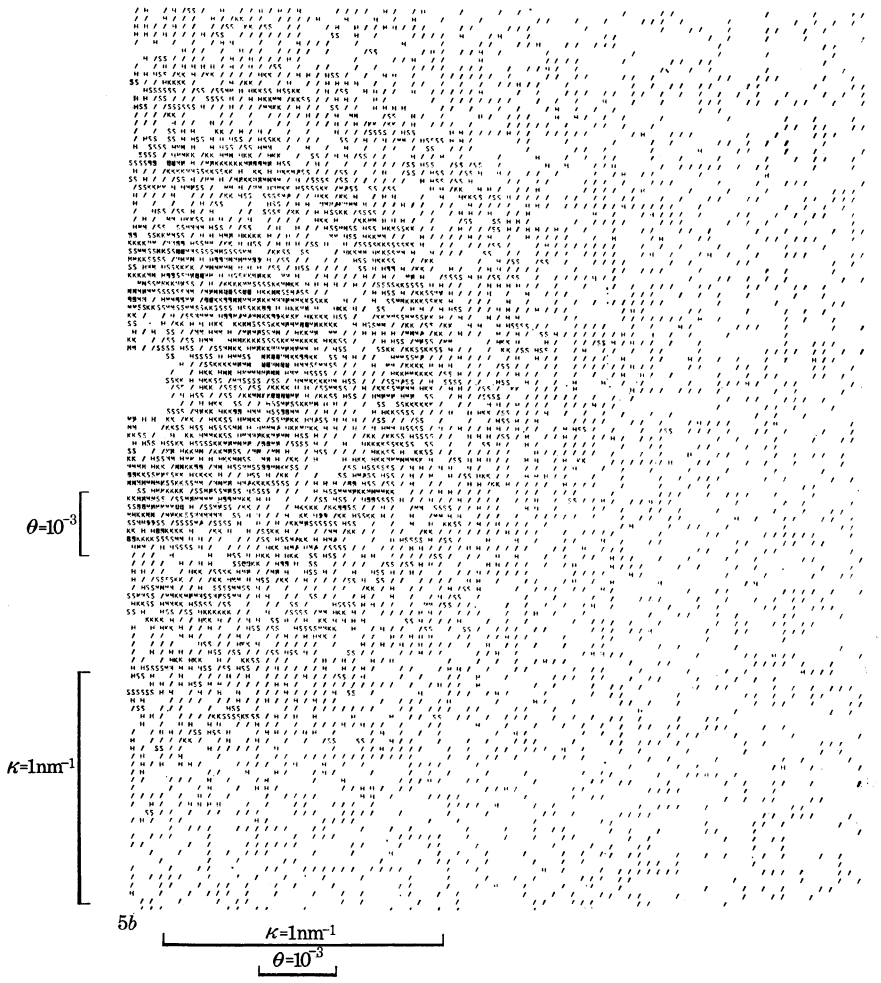

FIGURE 5. Squared Fourier transform of a strongly under focused image of an amorphous carbon foil. The micrograph of this carbon foil is one of the images which were used for the calculation of 'difference images' (figure 12). Figure 5*a* shows the light optical diffractogram of the micrograph, figure 5*b* a plot of the calculated squared Fourier transform of the image intensity. The wavelength of the electrons was $\lambda = 3.7$ pm, the spherical aberration $C_s = 3.9$ mm, the defocusing parameter, $z_0 = 410$ nm and the focal difference due to axial astigmatism, $\Delta f_A = 124$ nm.

PHILOSOPHICAL TRANSACTIONS OF THE ROYAL SOCIETY B BIOLOGICAL SCIENCES

research laboratory for electron microscopy (Thon 1966). Figure 5*a* shows an example of such a diffractogram; the nodes of the pupil function are immediately apparent.

Light diffractograms of electron micrographs were first used by Klug & Berger (1964) in their studies of the quarternary structure of biological macromolecules. But the above-mentioned work has an entirely different aim: not the structure of the object, but the electron optical parameters of the electron microscope are of interest. One of the first practical applica-

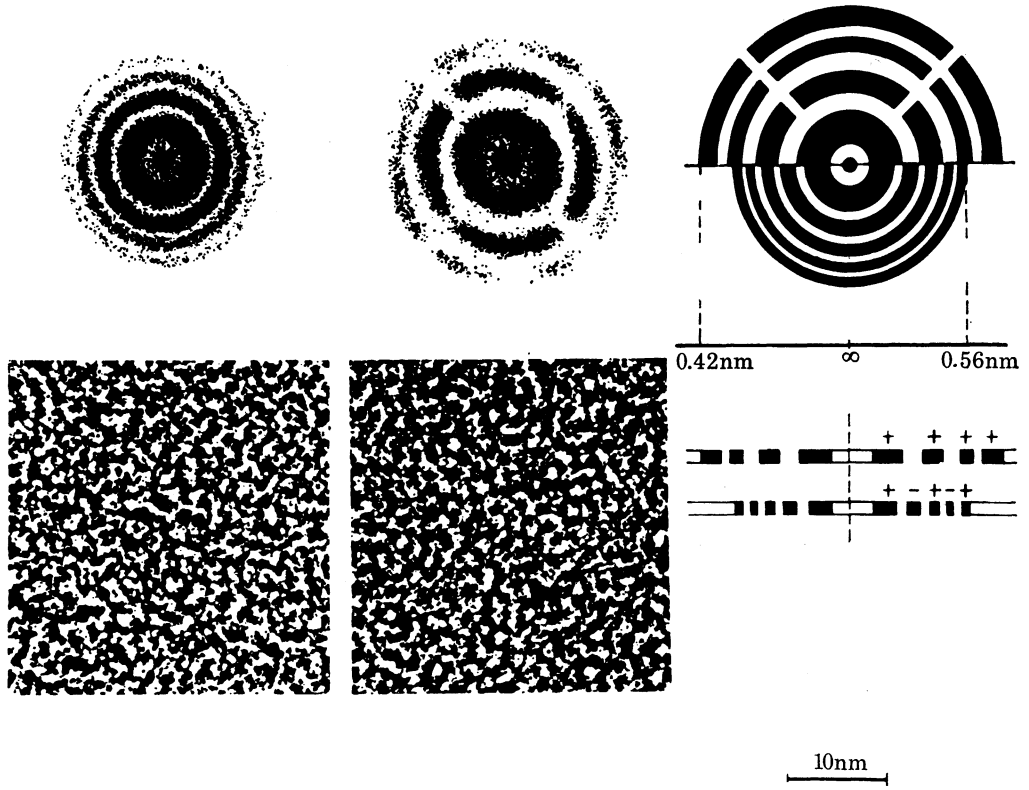

FIGURE 6. Electron micrographs of an amorphous carbon foil, taken without (on the left) and with the zone plate of figure 3 (on the right). The defocusing parameter was $z_0 = 480$ nm and $z_0 \approx 500$ nm respectively. The corresponding light optical diffractograms are shown on the top of the micrographs together with a schematic graph illustrating the synchronization of the annular zone screens with the corresponding zones of the pupil function.

tions of these principles concerned the adjustment of zone correction plates to the pupil function (Möllenstedt *et al.* 1968). Figure 6 shows the procedure; the Fourier transforms of a carbon foil with and without incorporated zone correction plates will be compared in order to achieve a synchronization of the annular zonal screens with the corresponding zones of the pupil function. (Of practical importance is a certain correlation between spherical aberration and defocusing. It allows compensation by a change of the focus for errors of the annular radii (caused by errors in C_s).) The knowledge of the optical parameters of an electron micrograph is of fundamental importance. It allows one to correlate the information registered on a micrograph with the potential distribution (the 'real structure') on a quantitative scale. This is naturally also important for work at lower resolution than atomic resolution. It is easy to understand that for quantitative work the handling of measured intensity data in a digital computer is more accurate than the conversion in light analogue devices. We have built an automatic scanning photometer with a resolution of few micrometres and have developed a

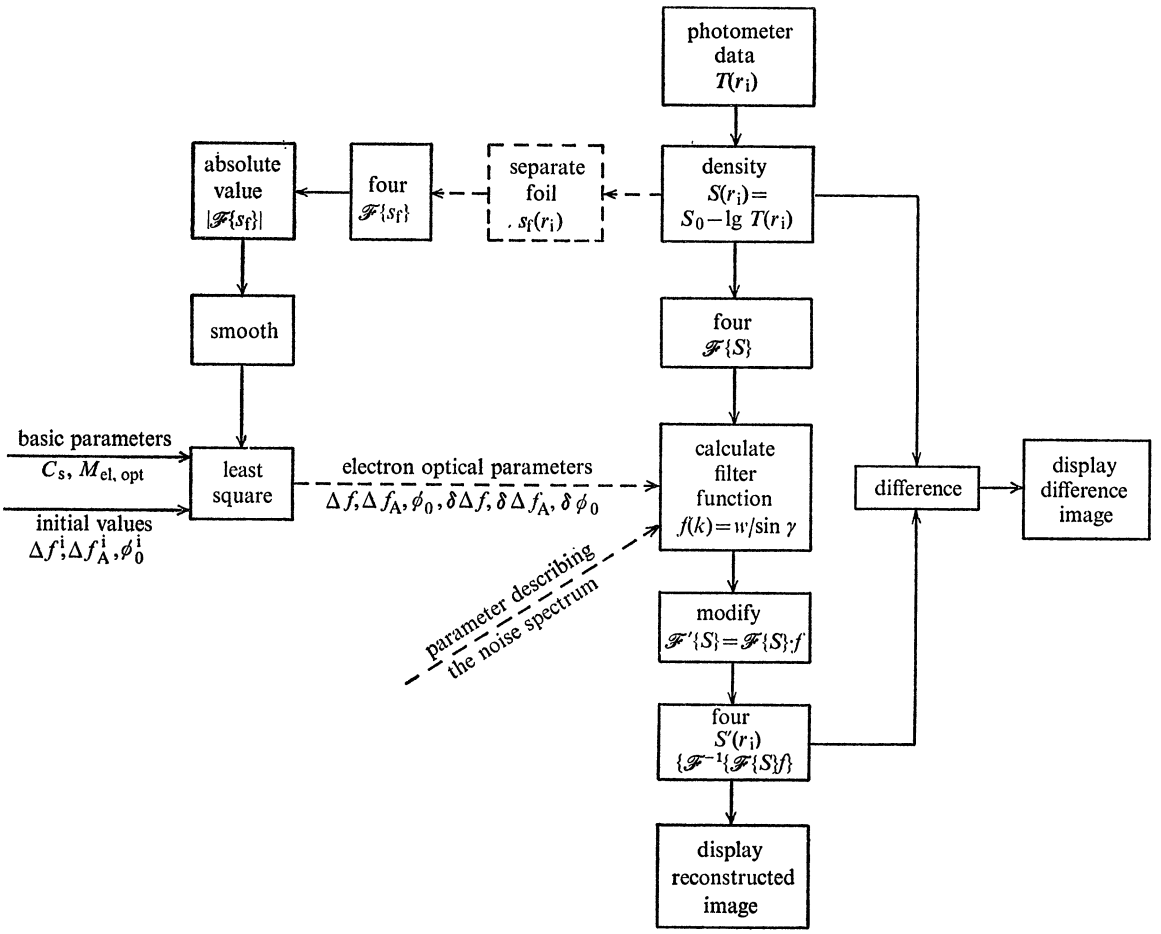

FIGURE 7. Computer program system for the calculation of the 'ideal image' (reconstructed image) from an image formed by a lens with spherical aberration, axial astigmatism and defocusing.

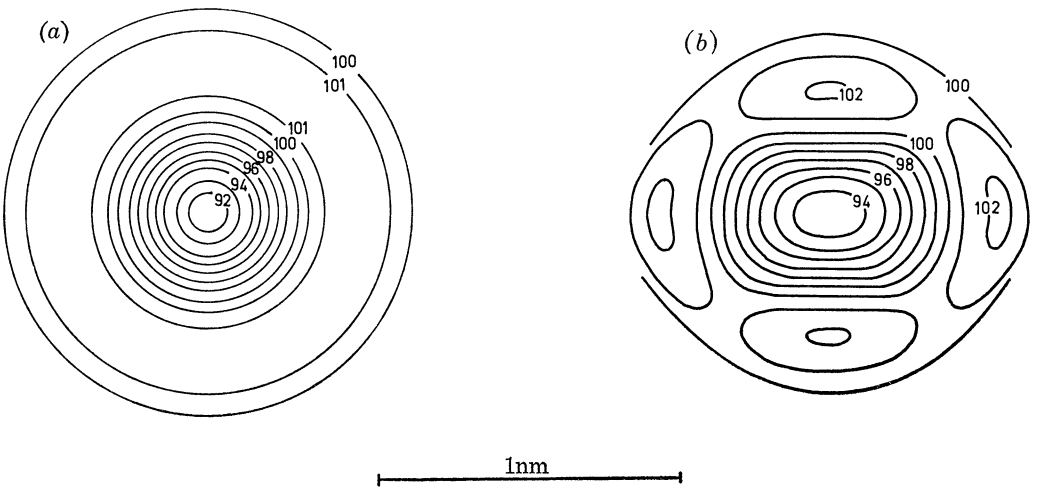

FIGURE 8. Calculated bright-field image of a single Hg atom with coherent illumination. The intensity of the primary beam is set to 100. Wavelength of the electrons $\lambda = 4.2$ pm (80 kV); spherical aberration $C_s = 3.9$ mm; defocusing parameter $z_0 = 120$ nm; objective aperture $\alpha = 0.01$ rad; the intensity distribution in figure 8*a* is the image without axial astigmatism, figure 8*b* with axial astigmatism, $\Delta f_A = 80$ nm (horizontal: $\Delta z_{eff} = z_0 - \frac{1}{2}\Delta f_A = 80$ nm; vertical: $\Delta z_{eff} = z_0 + \frac{1}{2}\Delta f_A = 160$ nm).

number of computer programs for an IBM 360/91, using very fast computer routines, etc. Figure 7 shows a block diagram of one of our program systems. Figure 5*b* shows a calculated 'pupil function'. Another advantage of computer data handling is that the optical parameters can be extracted from the density function (without additional measurements) and refined using least square principles. The results are surprisingly accurate, if one takes into account not only the nodes but also the shape of the Fourier transform. (In a special example ~ 3 nm in

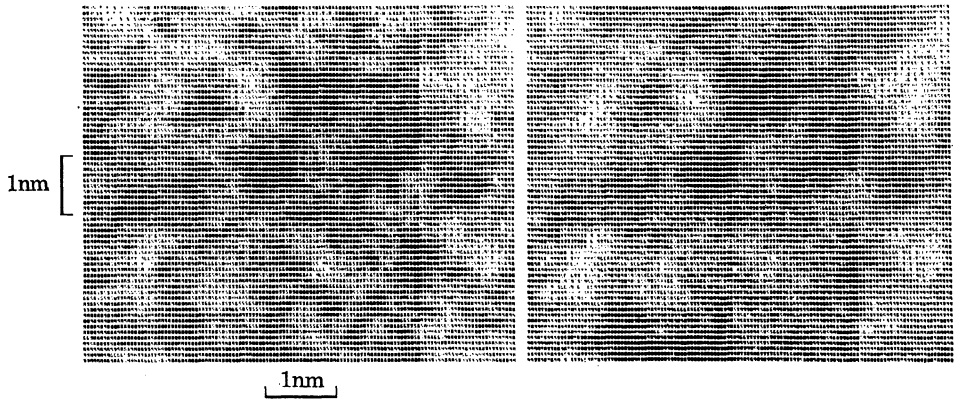

FIGURE 9. Calculated bright-field images of the murein-sacculus of *Spirillum serpens* (Gram negative bacterium); on the left the original image with the same electron optical parameters as the 'image point' of the Hg atom in figure 8*b*; on the right the reconstructed image, calculated with the computer program system illustrated in figure 7. The back-modifying function (filter function) was

$$\exp\,[C(1-1/|\sin\gamma|)]/\sin\gamma$$

(γ is the wave aberration)

defocusing and ~ 8 nm in axial astigmatism. It should be remarked that the optical parameters can also be extracted from the Fourier transform of the object itself though less accurately (important in the case of membrane structures etc).) It is, for example, possible to calculate the 'image point' for a micrograph. Figure 8*b* shows an image point in a micrograph of a membrane structure, taken near the Scherzer focus (defined in Scherzer (1949), see also Hoppe (1970*a*). It can be seen that the image point is distorted by axial astigmatism. Figure 8*a* shows how the undistorted image point would look. Note in figure 8*b* and 8*a* the positive regions around the maximum, predicted by Scherzer (1949), and now experimentally verified, due to the decrease of phase contrast at low scattering angles. If we characterize the resolution by the distance where a 75% depression occurs in the super-position of two image point functions (see, for example, Glaser (1952)), than the corresponding resolutions along the principal axes of axial astigmatism are 0.4 and 0.6 nm. The next step is the correction (reconstruction) of the image. (The use of the real part reconstruction scheme for electron microscopy has been proposed by Hanszen (1968) and Schiske (1968).) In the simplest case this correction means a sign change of the Fourier coefficients in the negative regions of the pupil function. A more complicated 'filter function' could also—at least partially—correct for the decrease near the nodes of the pupil function. Figure 9 shows a 'calculated' density function of the membrane with and without correction.

The theoretical basis of image reconstruction with special emphasis on structure determination at atomic resolution has been treated elsewhere (Hoppe 1970*a*); in the following we discuss only some interesting aspects.

PHILOSOPHICAL TRANSACTIONS OF THE ROYAL SOCIETY B BIOLOGICAL SCIENCES

The distorted 'structure factor' F' of the image amplitude ψ (produced by Fourier transformation of ψ) is

$$F'_{x^*,y^*,z^*} = S_0 \sum_j^n f_j \exp\{2\pi i\,(x^*x_j + y^*y_j + z^*z_j)\} \tag{2}$$

(f_j: atomic electron scattering factors; x_j, y_j, z_j: rectangular coordinates of the atoms; z^*: directed along the optical axis; n: number of atoms; x^*, y^*, z^*: reciprocal coordinates). z^* is connected with x^* and y^* by the formula

$$z^* = \tfrac{1}{2}\lambda\,(x^{*2} + y^{*2}). \tag{3}$$

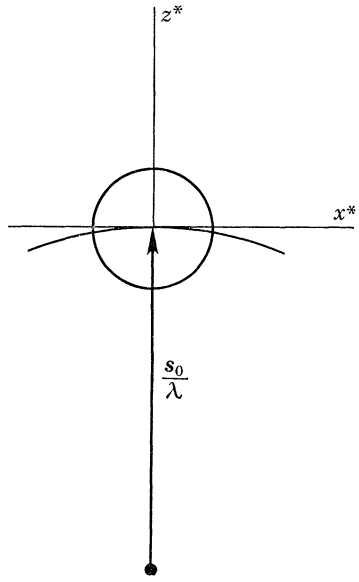

FIGURE 10. 'Diffraction geometry' in electron microscopy using the concept of the Ewald sphere. Wave vector $\boldsymbol{s}/\lambda$ of the illumination oriented along the optical axis z in this special case. The small circle (around the origin of reciprocal space x^*, y^*, z^*), indicates the three-dimensional resolution limit.

Equation (2) describes therefore a two-dimensional relation on a curved surface in the reciprocal space. This surface is the Ewald sphere. In fact as figure 10 demonstrates—electron microscopy with coherent illumination corresponds to a special case in diffractometry.

Of further interest is the function S_0. It can be understood as a generalized 'modifying function' (see Hoppe 1970). This function S_0 is related to the pupil function:

$$S_0 = \exp(i\gamma_0 + \tfrac{1}{2}\pi). \tag{4}$$

It is immediately clear that the product of (2) with a 'back-modifying function'

$$S_0^{-1} = \exp\{-(i\gamma_0 + \tfrac{1}{2}\pi)\} \tag{5}$$

delivers the undistorted structure factors F_{x^*,y^*,z^*}. Another important point is, that not only the uncorrected F'_{x^*,y^*,z^*} but also the corrected F_{x^*,y^*,z^*} lead to a complex amplitude in the image plane. This is evident if there are atoms with appreciable anomalous scattering (e.g. heavy atoms), but it is also true in the case of purely elastic scatterers due to the curved Ewald sphere ($F_{x^*,y^*,z^*} \neq F_{-x^*,-y^*,z^*}$).

It is easy to see that an actual density function can never be recorded as a complex Fourier function, at least if—as in conventional electron microscopy—no transformation of

variables takes place. (In some holographic techniques this can be done. See also Hoppe, Langer & Thon (1970)). This is the reason why only the real part of the image function can be seen in the (real) density function of the electron micrograph. One way out of these difficulties is to take more than one micrograph in different conditions. For example the scheme, proposed by Schiske (1968) for image reconstruction from a focal series can be used for the evaluation of the complex function. For the same purpose we have proposed a new reconstruction scheme (Hoppe *et al.* 1970) based on earlier experiments of one of us. This scheme uses micrographs

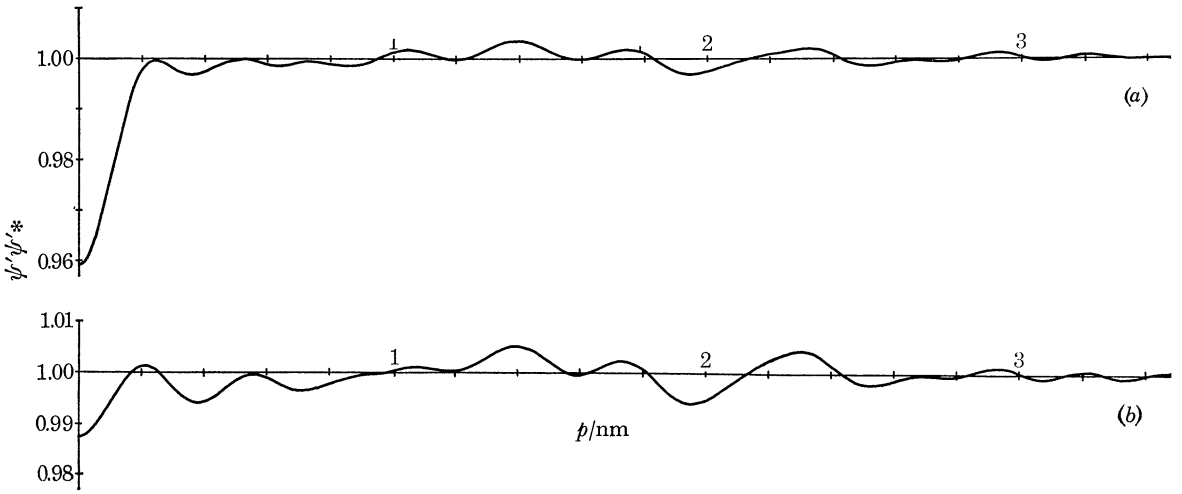

FIGURE 11. Calculated bright-field image of a single C atom with coherent illumination. The electron optical parameters are: wavelength of the electrons $\lambda = 3.7$ pm (100 kV); spherical aberration, $C_s = 4.7$ mm; defocusing, $z_0 = 560$ nm; objective aperture $\alpha = 0.014$ rad. In (*a*) a zone plate is used which is adapted to these electron optical parameters; (*b*) shows the image with the same parameters using no zone plate.

taken while screening off one half of the aperture by semicircular screens. It can be shown that with two exposures, taken with complementary semicircular screens, the complete complex information can be registered.

In comparison with the real part scheme the new scheme has the additional advantage that there is no depression of the Fourier coefficients at the nodes of the pupil function. As has been shown by Hoppe (1970*a*), one micrograph is sufficient to register the whole information in the case of a pure real (amplitude object) or imaginary (phase object) image function.

We come now to a comparison of both fundamental schemes of zonal correction. It is evident that image reconstruction schemes are experimentally very much simpler than schemes, where screens, phase foils, etc., have to be incorporated into the objective of an electron microscope. On the other hand, certainly the 'on line' creation of the image in the microscope is an advantage, especially if this image can be studied without loss of resolution using modern image intensifier, etc. on the screen.

One problem in image reconstruction needs special reference. Figure 11 shows the highly defocused 'image' point of a C atom, taken in the same microscope with and without insertion of a zone screen plate† corrected for phase contrast. It can be easily seen, that the maximal contrast in the latter case is very low. For reasons, which cannot be discussed here, this does not mean that the signal:noise ratio becomes worse! In the case of extended objects the contrast

† We propose to differentiate the different types of zone correction plates as zone screen plates, zone phase plates and continuous zone phase plates.

will be enhanced, because of the overlap of the diffuse atomic images. But difficulties on the border of the analysed object region will appear due to the cutting off of the diffuse image points (Hoppe 1970*a*). It goes without saying, that correction for chromatic errors (see Hoppe 1970*b* and other papers in the Hirschegg meeting) and partial coherence are necessary for quantitative work as well. Therefore adding as much intensity as possible into the regions near the image point might in any case be of advantage. Here perhaps a generalization of the resolution extending principle of zonal correction could offer new possibilities. The pupil functions discussed above have rotational or nearly rotational (in the case of axial astigmatism) pupil functions. Scherzer has shown (1949) that the introduction of elements with cylindrical symmetry can improve the pupil function in such a way that the characteristics of a nearly ideal lens are achieved. But systems of that kind turn out to be very complicated in design and alinement. The correction elements introduce new errors, which seriously restrict the useful image field. But one might ask, whether really a complete correction is necessary if zonal correction by image reconstruction is applied. (A partially corrected electron lens has been described by Scherzer & Typke (1967/8).)

The three dimensional object

Electron microscopy is essentially a two-dimensional procedure: 'Infinitely' thin objects are imaged in a two-dimensional micrograph. At low resolutions this concept works quite well. Micrographs at resolutions 2 to 100 nm of ultramicrotome sections can really be understood as images of thin slices cut through a three-dimensional body. But at atomic resolution such a procedure would be impossible. Even if a 'super ultramicrotome' could be built, which cuts sections of say 0.5 nm thickness, the internal structure of a biogenic macromolecule would be drastically altered by the cutting procedure. Crystal structure analysis has shown how to cope with 'thick' objects: diffraction experiments have to be organized in such a way that the structure factors (Fourier coefficients) in the three-dimensional reciprocal space (and not only on the surface of the Ewald sphere) are measured. The well known and obvious way in crystal structure analysis is to rotate the specimen. For electron microscopy equivalent schemes independently have been worked out by DeRosier & Klug (1968) and for the analysis of protein crystals by Hoppe, Langer, Knesch & Poppe (1968). For the quarternary analysis of the structure of negatively stained biogenic macromolecules at resolutions of about 2 nm this method has already been successfully applied (see other papers in this volume). For the analysis of protein crystals the progress has been rather slow, as the thin unstained sections are very sensitive to electrons. (The use of image intensifiers for this work might be helpful.) For high resolution work this method has not yet been applied. Some difficulties might be worth mentioning. In low resolution field the specimen—e.g. a virus particle—can be regarded as a finite three-dimensional body. The structure of the surrounding can be neglected. At atomic resolution the structure of the support must be taken into account. In some cases tilting schemes can be found, which cope with this difficulty (Hoppe 1969*b*). A really general solution is provided only by the image difference technique (see later). Another problem concerns the limitation of the tilting angles, which generates blind regions in the reciprocal space. In low resolution work particles have been studied, which are symmetrical within the limit of the resolution. Therefore the blind regions can be filled using symmetry considerations. (In the case of crystal structure analysis the elementary unit is the 'finite body'.) At high resolution asymmetry will be the rule; even in the

PHILOSOPHICAL TRANSACTIONS OF THE ROYAL SOCIETY B BIOLOGICAL SCIENCES

case of symmetric molecules the symmetry will certainly be distorted. One must not forget, that the reason for the surprisingly high symmetries in the case of crystals is the well-defined crystal field in the surrounding of the molecule. We shall come back to the problem of the limited tilting angle in the discussion of redundancy principles. A further experimental difficulty concerns the stability of the image conditions at different tilting angles. As far as the constancy of electron optical parameters (such as defocusing, change of axial astigmatism magnification, etc.) is concerned, the extraction of the physical structure using the image reconstruction schemes described above makes it unnecessary to keep these parameters extremely constant. At high resolution also the curvature of the Ewald sphere can be taken into account, if the complex image amplitude is measured. On the other hand, the requirements for stability of the physical object under the influence of the incident electrons are very high; three-dimensional imaging generally means a higher radiation loading than two-dimensional imaging.

For completeness of our analysis the discussion of 'partial three-dimensional imaging' is now necessary. A well-known scheme of this kind is stereoscopic imaging. It corresponds in reciprocal space to two projections, inclined to each other by a small angle. The additional three-dimensional information is not very great; in fact it would be impossible to unscramble a complicated three-dimensional density function from its stereoscopic view. A more promising scheme can be deduced from (2) and (3). Let us assume, that the F'_{x^*,y^*,z^*} have been corrected to the undistorted structure factors F_{x^*,y^*,z^*} and that wavelength and resolution have been chosen in such a way, that a substantial fraction of the Ewald sphere has been covered. As (2) corresponds to a three-dimensional function, a corresponding three-dimensional density function $\rho_{p,x,y,z}$ can be calculated, using a set of structure factors F_{p,x^*,y^*,z^*} which are related to the complete set of structure factors F_{x^*,y^*,z^*} by the relations

$$\left.\begin{aligned} F_{p,x^*,y^*,z^*} &= F_{x^*,y^*,z^*} \quad \text{for} \quad Z^* = \tfrac{1}{2}\lambda\,(x^{*2}+y^{*2}),\\ F_{p,x^*,y^*,z^*} &= 0 \qquad\quad \text{for} \quad Z^* \neq \tfrac{1}{2}\lambda\,(x^{*2}+y^{*2}). \end{aligned}\right\} \tag{6}$$

It is now convenient, to introduce the 'image point' $\rho_{i,x,y,z}$ of the partial three-dimensional image. In the example discussed here its Fourier transform ϕ_i is given by

$$\left.\begin{aligned} \phi_i &= 1 \quad \text{for} \quad Z^* = \tfrac{1}{2}\lambda\,(x^{*2}+y^{*2}),\\ \phi_i &= 0 \quad \text{for} \quad Z^* \neq \tfrac{1}{2}\lambda\,(x^{*2}+y^{*2}). \end{aligned}\right\} \tag{7}$$

In the case of the complete three-dimensional image the Fourier transform is simply $\phi = 1$ for all structure factors within the resolution sphere; the corresponding image point is a delta function. If $\rho_{x,y,z}$ denotes the undistorted three-dimensional function, then it follows from (6) and (7):

$$F_p = \phi_i F, \quad \rho_p = \rho_i^* \rho. \tag{8}$$

In our case the 'image point' has a twin-cone structure with rotational symmetry. It must be mentioned, that the 'image point' is complex; ϕ_i in (7) does not obey the Friedel law. But if the structure factors F_{x^*,y^*,z^*} themselves obey the Friedel law (e.g. in the case of pure amplitude or phase objects or objects consisting only of one kind of atoms),

$$(|F_{-x^*,-y^*,-z^*}| = |F_{x^*,y^*,z^*}|),$$

then (7) can be replaced by

$$\left.\begin{aligned} \phi_i &= 1 \quad \text{for} \quad Z^* = \pm\tfrac{1}{2}\lambda\,(x^{*2}+y^{*2}),\\ \phi_i &= 0 \quad \text{for} \quad Z^* \neq \pm\tfrac{1}{2}\lambda\,(x^{*2}+y^{*2}), \end{aligned}\right\} \tag{9}$$

and the image point function becomes real. If substantial anomalous scattering is present, (9) can be applied if for example a second half screen image pair (Hoppe *et al.* 1969*a*) has been taken with a tilt of the specimen of 180°.

PHILOSOPHICAL TRANSACTIONS OF THE ROYAL SOCIETY B BIOLOGICAL SCIENCES

The 'partial three-dimensional scheme' discussed above is a generalization of the 'focusing through' principle of light optical imaging with objectives with high aperture. From the work in light optics it is known, that this principle can very simply be applied in coherent bright field image reconstruction. In a thick object the focal plane can be changed at will by a change of the defocusing parameter in the back-modifying function (5). If one calculates several image reconstructions with different focal parameters one gets therefore a 'through focus' series. In the following it will be shown, that also in this case a 'partial three-dimensional function' can be established. We write (2) in the form

$$F'_{x^*,y^*,z^*} = S_0 \sum_j^n f_j \exp(2\pi i z^* z_j) \exp\{2\pi i (x^* x_j + y^* y_j)\}. \tag{10}$$

The image amplitude ψ, calculated by the Fourier synthesis of (10) is complex; corresponding to (1) (third term neglected) only the real part of ψ can be registered. If we assume, that the structure ρ to be studied consists of atoms with constant anomalous scattering (e.g. negligible anomalous scattering or a structure with equal atoms), the structure factors F' and F'^*, of ψ and ψ^* respectively, can be written as:

$$\left.\begin{aligned} F'_{x^*,y^*,z^*} &= S_0 \exp(i\epsilon_0) \sum_j^n f_j \exp(2\pi i z^* z_j) \exp\{2\pi i (x^* x_j + y^* y_j)\}, \\ F'^*_{x^*,y^*,z^*} &= S_0^* \exp(-i\epsilon_0) \sum_j^n f_j \exp(-2\pi i z^* z_j) \exp\{-2\pi i (x^* x_j + y^* y_j)\}, \end{aligned}\right\} \tag{11}$$

ϵ_0 = phaseshift of anomalous scattering.

A Fourier analysis of the micrograph therefore reveals Fourier coefficients F'', which are proportional to the sum of F' and F'^*. We introduce now as a back-modifying function the function σ_0†

$$\sigma_0 = S_0 \exp(i\epsilon_0) + S_0^* \exp(-i\epsilon_0). \tag{12}$$

The product of (11) and (12)—the result of the image reconstruction—can be written as

$$\begin{aligned} \sigma_0 F'' = (\cos\alpha + 1) \sum_j^n f_j [&\exp\{2\pi i (x^* x_j + y^* y_j + z^* z_j)\} + \exp\{2\pi i (x^* x_j + y^* y_j - z^* z_j)\}] \\ + i \sin\alpha \sum_j^n f_j [&\exp\{2\pi i (x^* x_j + y^* y_j + z^* z_j)\} - \exp\{2\pi i (x^* x_j + y^* y_j - z^* z_j)\}] \end{aligned} \tag{13}$$

with

$$\left.\begin{aligned} \cos\alpha &= \tfrac{1}{2}\{S_0 \exp(2i\epsilon_0) + S_0^{*2} \exp(-2i\epsilon_0)\}, \\ i \sin\alpha &= \tfrac{1}{2}\{S_0^2 \exp(2i\epsilon_0) - S_0^{*2} \exp(-2i\epsilon_0)\}. \end{aligned}\right\} \tag{14}$$

The first term corresponds to a partial three-dimensional image similar to that discussed in (8), consisting of 'atoms' with the 'scattering power' f_j $(\cos\alpha + 1)$ but with a superposed mirror image (mirror plane = focusing plane) of the object. The second term has an oscillating 'scattering factor' $if_j \sin\alpha$ (image and mirror image with opposite weight) and generates therefore additional noise. (One might be puzzled by the fact, that 'imaginary atomic scattering factors' formally occur in (13). The answer is, that they are necessary to retain the 'Friedal law' in the non-Friedel pair F'_{x^*,y^*,z^*} and $F'_{-x^*,-y^*,-z^*}$.) If the focusing plane is outside the object, a two-dimensional section of (13) through the object image will therefore show only those atoms as 'focused', which belong to that section. Equation (14) leads to the important conclusion, that the focal plane should be adjusted to be outside the object in order to separate image and mirror image.

† If a modifying function is proportional to the real part $(S+S^*)$ of a complex function S, then the product $(S+S^*)$ $(S+S^*)$ is everywhere positive. Therefore $(S+S^*)$ is also a back-modifying function.

PHILOSOPHICAL TRANSACTIONS OF THE ROYAL SOCIETY B BIOLOGICAL SCIENCES

The image difference method

This method has the aim of correcting for the structure of the 'support' in a general way. One important aspect of this work is that very small objects—in principle even single atoms—can be studied. The reason is that the resulting image corresponds to the difference between the structure of support and object and the structure of the support. For the study of small molecules two-dimensional methods might already be sufficient. For the study of three-dimensional structures the image difference method might provide the necessary 'zero surrounding' for an accurate mathematical analysis. One could perhaps discriminate between physical and chemical image difference methods. A typical physical method is the use of complex image functions for the separation of atomic images (Hoppe *et al.* 1970*a*); we have already discussed ways to register the complex function in this paper. This method would be especially suited to the discrimination of single heavy atoms.† For the practical use of this method it is very important that electron anomalous scattering is much higher than X-ray anomalous scattering. For example for 40 kV electrons the phase shift for Hg changes from about 20 to about 70° in the region of 0.09 nm resolution! The corresponding change for light atoms is from about 2 to about 20°.

Also the discrimination of the image of a thin crystal (used as a supporting film) against the image of the object (by image reconstruction) might be regarded as 'physical'. The chemical methods work with at least two different exposures and an interconnected chemical process. The 'difference' can be created by 'addition' or 'subtraction'. Of special importance are gas reaction methods, especially if they can be used in the microscope itself. In the latter case the difficult procedures of taking the specimen out and inserting it again into the microscope can be avoided. Gas reaction methods can be used for subtraction and addition. One example of a subtraction method is the removal of an organic specimen by oxidation (e.g. under the influence of the incident radiation) after the (two-dimensional or three-dimensional) exposures. For this purpose thin supporting films are being developed in our laboratory, which are resistant to oxidation. Additive and subtractive gas reaction can be used for the study of reaction products. One interesting case is the reaction of organic material under the influence of incident electrons. These reactions take place in every electron microscope and cause, for example, the unwanted deposit of organic reaction products on the specimen. Experiments of this type are extremely important as they concern the physical stability of specimens in general. We have started chemical difference image experiments using a carbon foil (10 to 20 nm thick) as specimen. Figure 12 shows the first preliminary results. By adjusting a quite large (and constant) defocusing in both exposures, distorted images have been produced; distorted and reconstructed difference images have been calculated. Regions with no change can be recognized by the small contrast in the distorted difference image. The necessary image reconstruction can obviously be done before or after the calculation of the difference. The first procedure is necessary if the electron optical parameters have changed between both exposures. Of importance are methods which bring the two exposures to be subtracted into exact coincidence. For

† A method based on the different weight of atomic peaks, imaged by the elastically or inelastically scattered radiation has been worked out by Crewe, this volume, p. 61. The latter method leads to restrictions at high resolutions, as the image Fourier transform for inelastic scattering is limited to small scattering angles (low image resolution, based on the physical process of inelastic scattering); therefore the important separation of the higher order Fourier coefficients of the light atom structure from the Fourier coefficients of the heavy atom structure cannot be done. With anomalous scattering only elastic scattering is used, and this delivers high order Fourier coefficients in the imaginary part as well as in the real part.

PHILOSOPHICAL TRANSACTIONS OF THE ROYAL SOCIETY B BIOLOGICAL SCIENCES

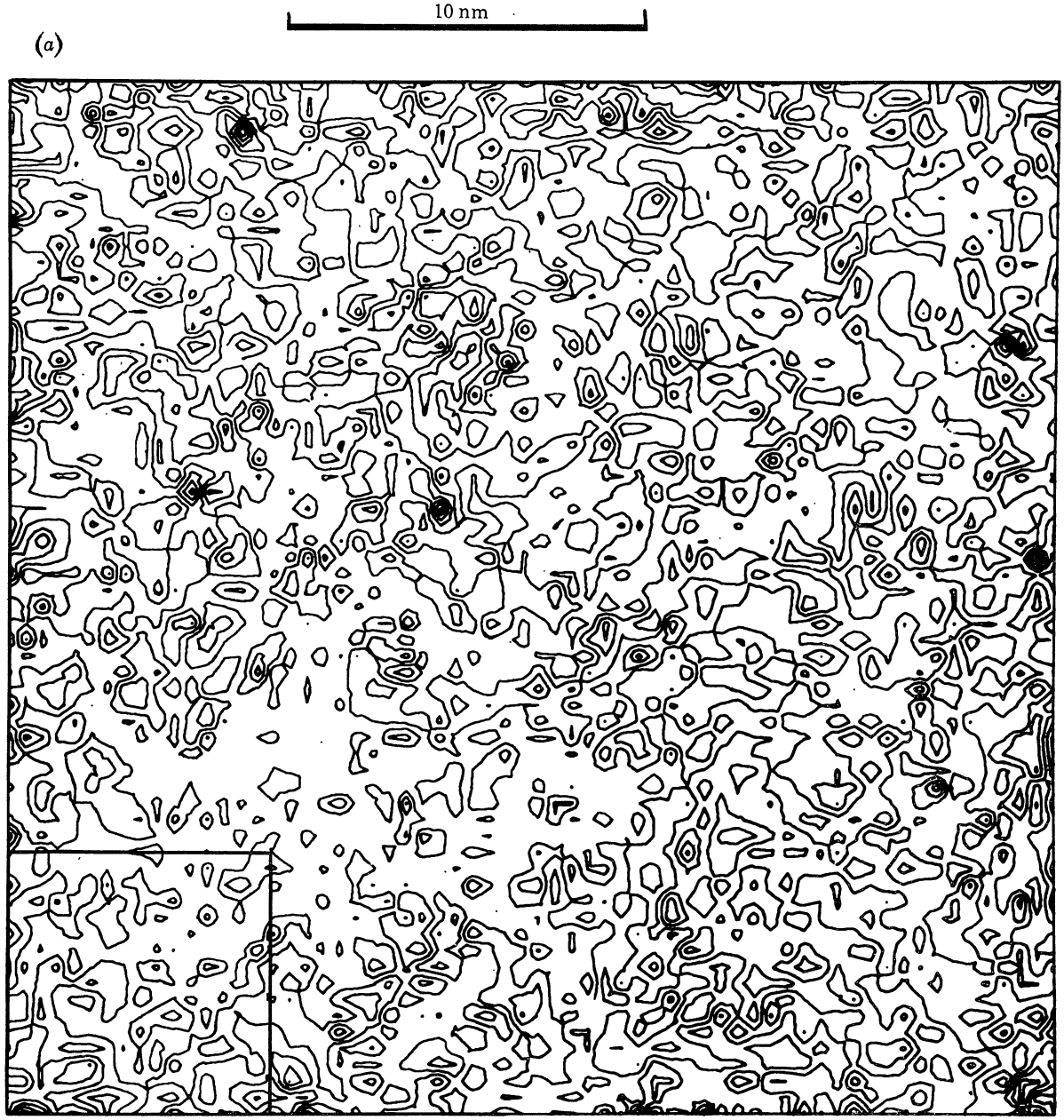

FIGURE 12. Difference image of an amorphous carbon foil, 10 to 20 nm thick. The two original micrographs were registered with the same electron optical parameters ($\lambda = 3.7$ pm, $C_s = 3.9$ mm; $z_0 = 410$ nm, $\Delta f_A = 124$ nm) at a magnification of 180000 on photographic films. The difference image shows the change of the foil after an electron bombardment of 80000 to 110000 electrons pers square nanometre in the microscope. The total pressure of the residual gases in the microscope (Elmiskop Ia) was about 10^{-5} Torr (13 μN m^{-2}); the specimen was surrounded by a chamber cooled down to liquid nitrogen temperatures. In (*a*) the difference between two successive lines of equal intensity corresponds to a step $\Delta S = 0.05$ of the registered optical density; lines of positive and negative values are not distinguished. The resolution of the map is 0.45 nm, i.e. for mapping all Fourier coefficients with $d^* = (1/d) > (1/0.45$ nm) were set to zero. In the lower corner on the left of figure 12*a* the region is marked which is shown in figure 12*b* in more detail: resolution 0.3 nm, difference between two successive lines of equal optical density $\Delta S = 0.03$. High maxima are marked by the symbols A0, A1,..., E9, A0 denoting the highest value and so on; low minima are marked by the symbols V0, V1,..., Z9, starting with the lowest value V0. (*c*) finally shows the reconstructed difference image of (*b*) using the same contour level distances as in (*b*).

PHILOSOPHICAL TRANSACTIONS OF THE ROYAL SOCIETY B BIOLOGICAL SCIENCES

this purpose correlation methods can be used, which are analogous to the 'convolution molecule methods' used to find known atomic groups in crystal structures (Hoppe 1957). In fact, the problem is equivalent: One has to find the image of the supporting film within the image of film plus specimen. Figure 13 shows two examples of the correlation functions used. Of special interest is the cross-correlation function (figure 13*b*), which delivers immediately the shift of both images. Note the surprising high accuracy of the shift parameters: < 0.1 nm recognizable in the sharpness of the correlation peak.

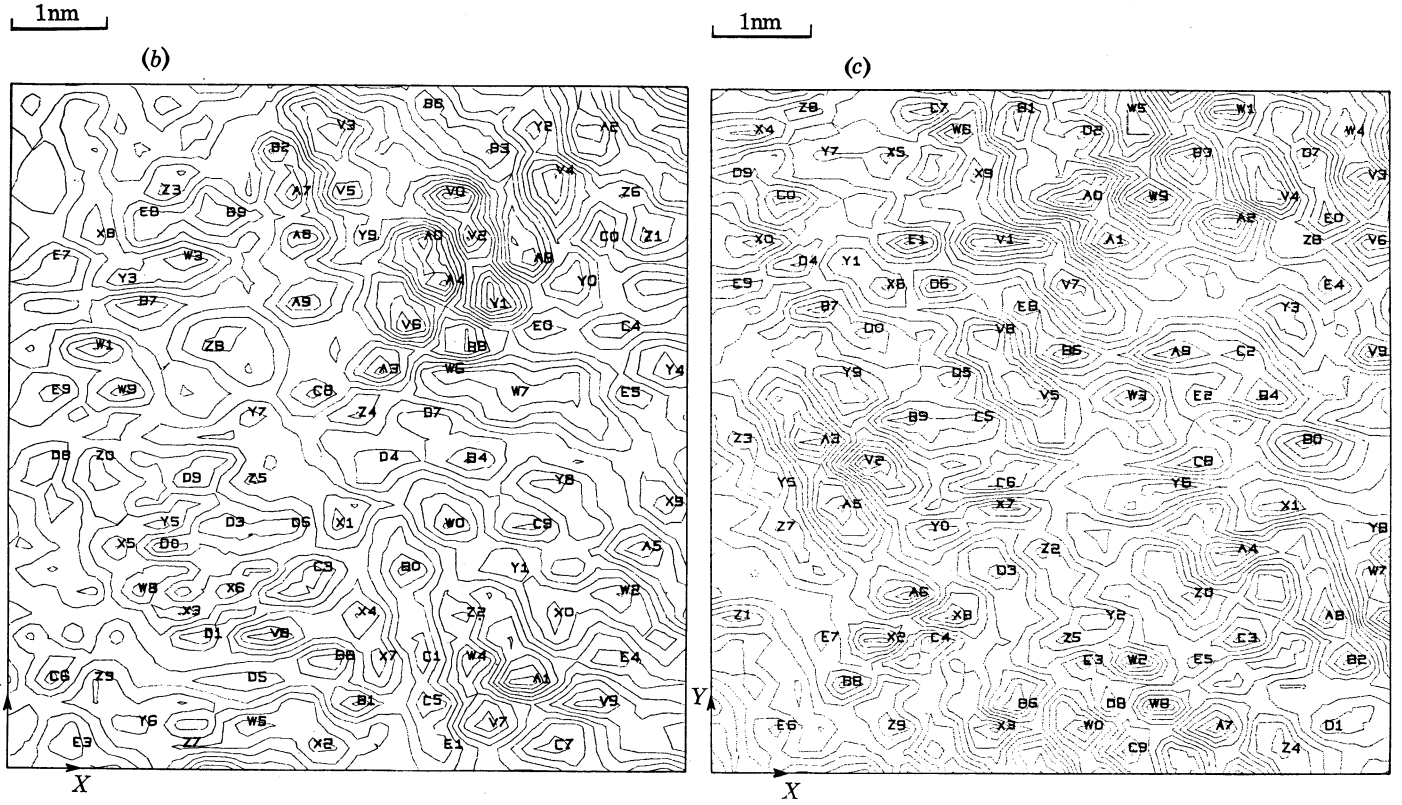

FIGURE 12*b* and *c*. For legend see previous page.

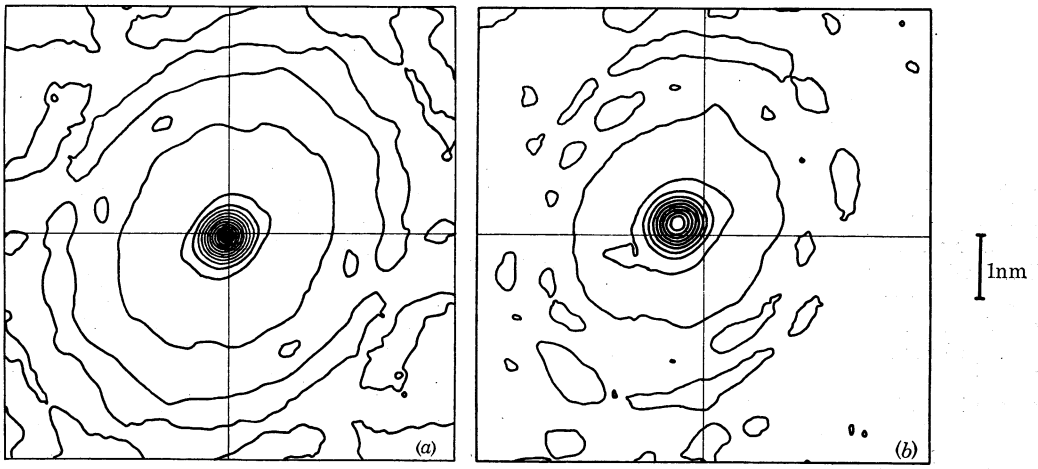

FIGURE 13 (*a*) Auto- and (*b*) cross-correlation function of the two images from which the difference image in figure 12*a* was calculated. The position of the cross-correlation peak in (*b*) denotes the translation vector of the two original images.

PHILOSOPHICAL TRANSACTIONS OF THE ROYAL SOCIETY B BIOLOGICAL SCIENCES

PHILOSOPHICAL TRANSACTIONS OF THE ROYAL SOCIETY B BIOLOGICAL SCIENCES

The redundancy principle

The criticism has been made (Hanszen & Morgenstern 1965) that an electron lens, corrected with a zone correction plate, could not show a 'real' enhancement of resolving power, as a substantial part of the spatial frequencies will be screened off. If one uses the well-known criterion for the definition of resolving power as the distance of two just separated image points, this statement is certainly wrong. But on the other hand it is true that image information is partly missing; this must influence the image. The answer can be found, if one compares the image point with the image point of an ideal lens (Langer & Hoppe (1966/7). In both cases there are weak and uniformly distributed ripples in the background of the image points; but the ripples are relatively higher in the case of the lens equipped with a zone correction plate. (A similar increase of noise will be found in the case of real part image reconstruction.) In both cases the noise is quasi randomly distributed. It will therefore usually be neglected. (In the case of coherent illumination the amplitudes of the noise add up; in the case of incoherent illumination the squares of the (small) amplitudes have to be added. Therefore the noise in the image is reduced in the latter case. The principle of Schlieren imaging with complementary zone correction plates (Riecke 1964; Langer & Hoppe 1967*b*) retains this advantage. But a general theory of structure determination has to discuss all sources of information loss due to the different schemes of data collection. This question again becomes critical for three-dimensional imaging procedures. It has already been mentioned that limitations in the experimentally obtainable tilting angles generate blind regions in the reciprocal space.

It is interesting to note, that information loss has already played a role in diffraction theory. In X-ray crystal structure determination one half of the information—the phases—will be lost. The general answer is that the lost information can be generated by calculation, if some features of the structure are known in advance. The information, provided by the Fourier transform, then becomes redundant and a partial knowledge of this transform is sufficient to develop the whole transform. It might therefore be fruitful to pose the question in our case in a similar fashion: which structural features must be known, if a complete Fourier transform has to be developed from the only partially measured transform? It goes without saying that the information loss in our case is of a different kind; it is not the phases of the measured Fourier coefficients, but the amplitudes and phases of the unmeasured parts of the Fourier transform that are unknown.

At this point it must be remarked that a redundancy principle has already been discussed in optics some time ago. If an object is limited in space, then only the Fourier transform of a reciprocal lattice must be known, which corresponds to a lattice with a unit cell not smaller in its dimensions than the finite object. The information between the reciprocal lattice points is redundant. The Whittaker–Shannon theorem (Whittaker 1915; Shannon 1949) allows calculation of this information: further it generally allows—as an interpolation scheme—the regeneration of the Fourier transform, if only some parts are known. The application to the regaining of information loss due to zone correction plates or to gaining of information for the reciprocal space regions between exposures at discrete tilting angles in the three-dimensional case is obvious. On the other hand, the Whittaker–Shannon theorem is also an extrapolation theorem. In fact, it can be shown that the data in an unlimited Fourier space can be calculated, if only one part of it is known (Harris 1964). Unhappily this simplest way to atomic resolution—it is in principle possible even with light—is not practicable for several reasons. Even a less

ambitious scheme of extrapolation to the blind regions in the three-dimensional case (Hoppe 1969*b*) will probably lead to serious difficulties.

It might be asked whether other redundancies exist as well. For phase determination in X-ray crystal structure analysis the Whittaker–Shannon principle cannot be used, because the experiments deliver exactly the minimal information necessary for the image of the finite unit cell; there is no redundancy. (For an application of the Whittaker–Shannon principle for phase determination in electron diffraction see Hoppe 1969*a*.) Phase-determination procedures in crystallography use as redundancies the positivity of the electron density function, and the composition of this function of resolved atomic electron density peaks. These principles are also valid in electron diffraction. (Strictly speaking only if one neglects anomalous dispersion. But in the case of complex functions it can be used for the real and imaginary parts separately, if the anomalous shifts do not exceed about 90°. This condition is certainly fulfilled (in contrast to neutron diffraction!).) We have checked its applicability for regaining of Fourier information in the blind regions. The test example in figure 14 is taken from crystallography. The reciprocal lattice of a molecular structure (phorbol: $P2_12_12$, 20 C atoms, 60 atoms in the asymmetric unit (Hoppe *et al.* 1969*b*)) has been divided into spherical equidistant shells (thickness of the shells: about mean lattice constant). The structure factor in every second subsequent shell has then been set to zero. A Fourier synthesis of this partial reciprocal lattice leads again to the structure but with a higher background. The result of this experiment is a direct proof of the statement, that the 'minimal information' (corresponding to the Whittaker–Shannon theorem) is redundant corresponding to the known structural features in an electron density function at atomic resolution.† The next step was then the calculation of the missing Fourier coefficients. For this purpose we used our 'phase correction scheme' (Hoppe & Gassman 1968). Three cycles revealed the complementary structure factors in amplitude and phase with the surprising accuracy of about 8 %.

In our next model calculations we tried to use this redundancy principle for the replacement of the Fourier coefficients in the blind regions of a three dimensional reconstruction. We assumed a 'tilting angle' range of only $\pm 25°$. Again we have chosen a molecular crystal structure as an example (ingenol: $P2_12_12_1$, 26 C atoms, 8 O atoms, Zechmeister, Brandl & Hoppe 1969). The calculations have been done in three dimensions; they will be presented in projection only. (Computer drawn diagrams with a sample lattice 0.033 nm $\times$ 0.033 nm, linear interpolation.) Figure 15*c* shows the projection along the z axis (resolution equivalent to Cu Kα-radiation: *ca.* 0.08 nm). The circular shape of non-superposed atoms is recognizable. Figure 15*a* shows the same structure with the 'tilting reduction' of $\pm 25°$. The twin cone axis of the blind regions is parallel to the x^* axis. A smearing out of the structure along x takes place. (In the three-dimensional Fourier synthesis evidently this effect is less pronounced; nevertheless superpositions of atoms along x occur frequently.) Figure 15*b* shows the structure after the replacement of the missing structure factors by 'phase refinement' in three cycles. The regain of information (compare with figure 15*c*) is immediately apparent. (In three dimensions this regain appears even more pronounced.)

† It is well known, that a Fourier synthesis of 5 to 10 % of the strongest structure factors in most cases reveals at least the principal features of the atomic structure. But this type of information reduction is of a fundamentally different nature: it corresponds to a weighting function for the Fourier amplitudes ('small' amplitudes below a limit will be set to zero). It can be easily shown, that not all selection rules for the Fourier coefficients to be omitted lead to a preservation of the information. For example, if one omits the structure factors with $h = 2n+1$ the Fourier synthesis contains two superposed structures and therefore the double number of atomic peaks.

PHILOSOPHICAL TRANSACTIONS OF THE ROYAL SOCIETY B BIOLOGICAL SCIENCES

In the preceding chapter we have discussed the principle of 'partial three-dimensional analysis' with micrographs taken under conditions where the curvature of the Ewald sphere is significant. The 'image point' in this case has a twin cone structure. It would be naturally extremely interesting, if conditions could be found where the use of our redundancy principles could develop the complete reciprocal space within atomic resolution. It would mean that three-dimensional analysis could be done without tilting the specimen. If wide apertures could be applied, such a scheme would not be hopeless. But here the short wavelength of electrons at commonly used accelerating potentials is a disadvantage: the curvature of the Ewald sphere becomes large at scattering angles where the atomic form factors become very small. Let us summarize: at three-dimensional atomic resolution the peculiar structure of the 'image' allows

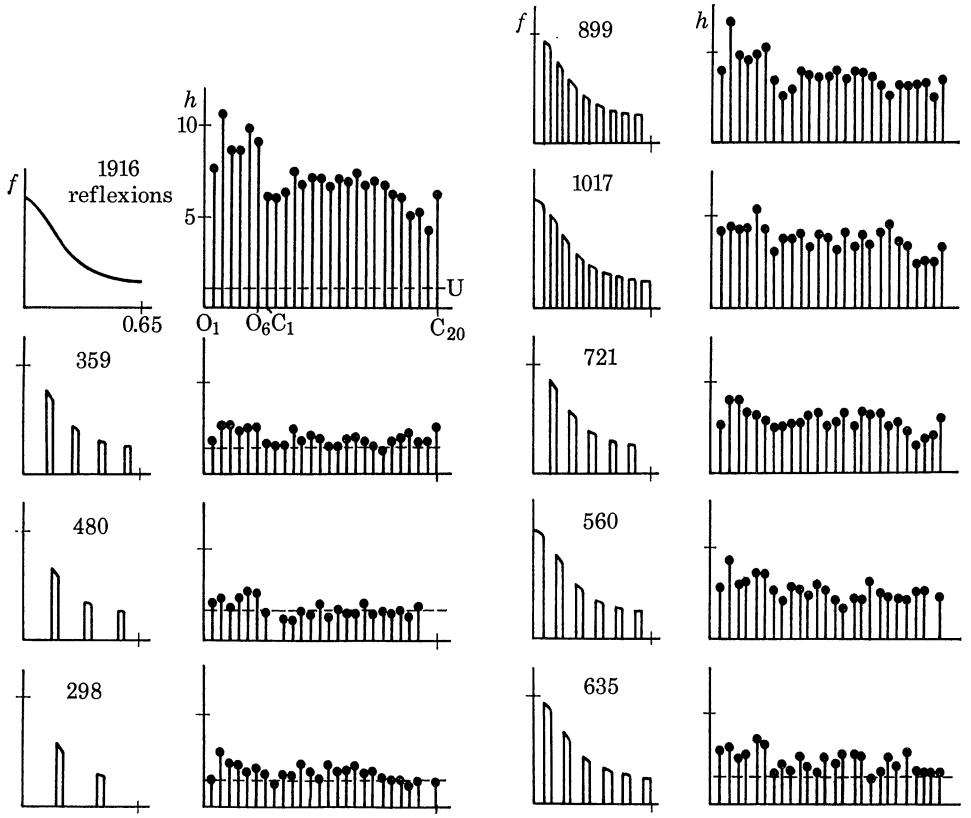

FIGURE 14. The graphs show the heights h of the atomic peaks in various maps of the electron density in the crystal structure of phorbol (6 O atoms, 20 C atoms). U is the level of the highest background peak. For their calculation the reciprocal space was divided in concentric spherical shells (radius sin θ/λ) and only the Fourier coefficients within the indicated shells were used for the Fourier synthesis of the electron density. The numbers '1916, 359, . . .' are the numbers of all reflexions within the shells. The figure shows calculations with very different numbers of reflexions. Note, that with shells of equal thickness (1017 reflexions or 899 reflexions) all atoms are above the limit of the highest background peak.

the use of the powerful 'atomic shape' redundancy principle, which already has been proved successful in crystal structure determination. But there might be one difficulty: if structural changes take place during the analysis, the 'atomic peaks' will lose their characteristic shape. It can be hoped, that at least a partial regain of information will be found if a substantial part of the structure has not been altered.

PHILOSOPHICAL TRANSACTIONS OF THE ROYAL SOCIETY B BIOLOGICAL SCIENCES

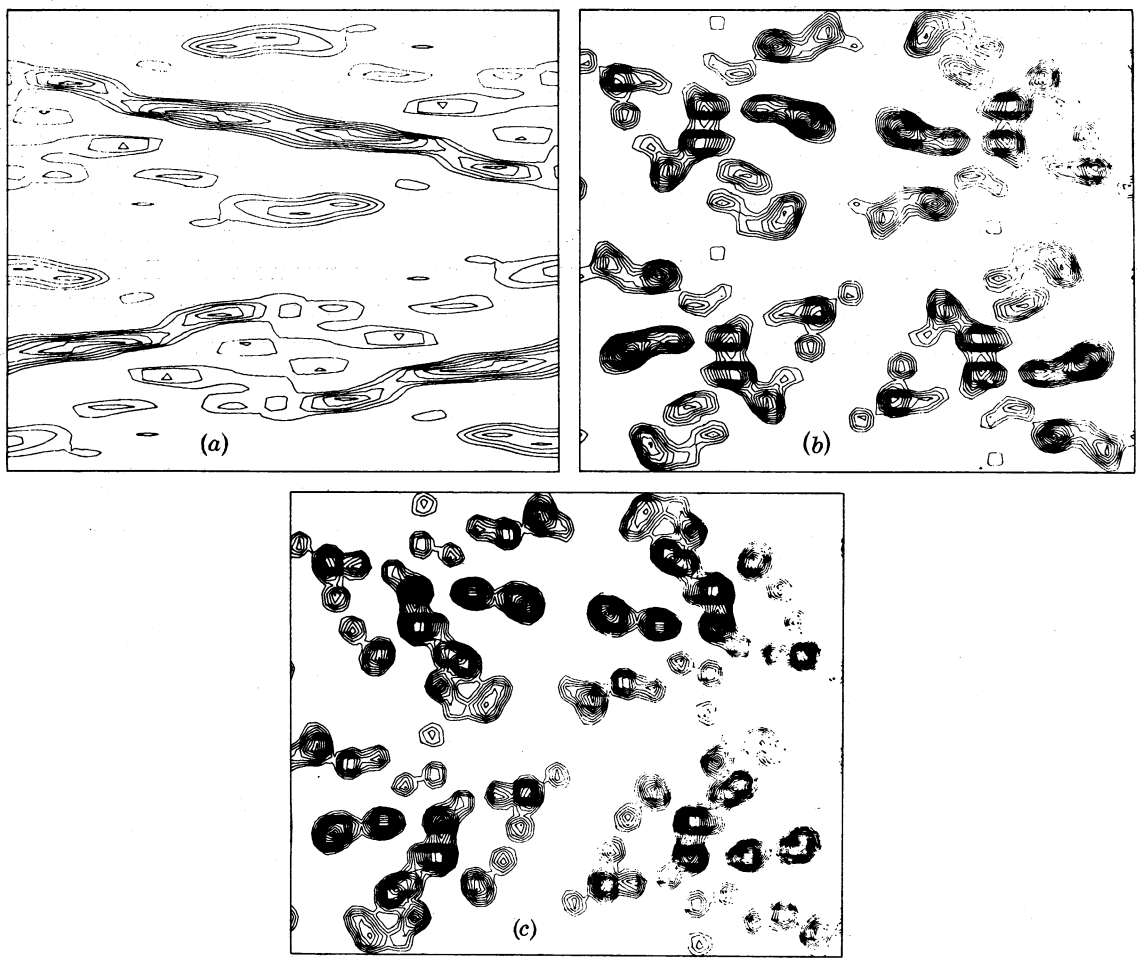

FIGURE 15. Contour maps of c-projections of inegol (a axis horizontal, b axis vertical). In (a) only the Fourier coefficients lying in a twin cone of $2\alpha = 50°$ (cone axis = b axis) are used for the calculation of the electron density. (b) shows the projection the Fourier coefficients out of the twin cone being calculated by 'phase refinement' (three cycles) from those within the cone. Compare these maps with (c), in which all measured Fourier data were used for the calculation of the electron density.

EQUIPMENT FOR HIGH RESOLUTION STUDIES

The experiments described in this paper have been done using a conventional Elmiskop Ia installation. At atomic resolutions the secondary errors become very important. In order to keep them as low as possible we have built a special installation in a place with no traffic in the neighbourhood, with low earth vibrations and low magnetic noise. The instrument has been equipped with a high potential set and a lens current supply having stabilities of better than 10^{-6} for periods of hours using an Elmiskop 101 as the basic microscope. There is little known about the specifications necessary for low vibrational and magnetic noise; they depend very much on the stiffness and the instrument used. Obviously of importance for such work are criteria for the image quality. The usual high resolution criterion in electron microscopy (minimal point distances) is worthless, because this criterion has no sense in distorted images. What we need is the limit of the Fourier space. If phase with contrast illumination along z (see figure 10) will be applied, this limit will be given by the Fourier transform of the image, no matter whether this image is distorted. Due to noise or various kinds, this limit is obscured. But

if one takes several exposures of the same object, the significant details can be separated by correlation functions. One of the simplest functions of that kind corresponds to the Fourier transform of the sum of two slightly displaced exposures of the same object taken under the same (or nearly the same) conditions. This function is modulated by a wave; the wave vector is parallel to the displacement, its length is proportional to the amount of the displacement. It is advantageous, that this function can easily be generated in a light diffractometer, inserting

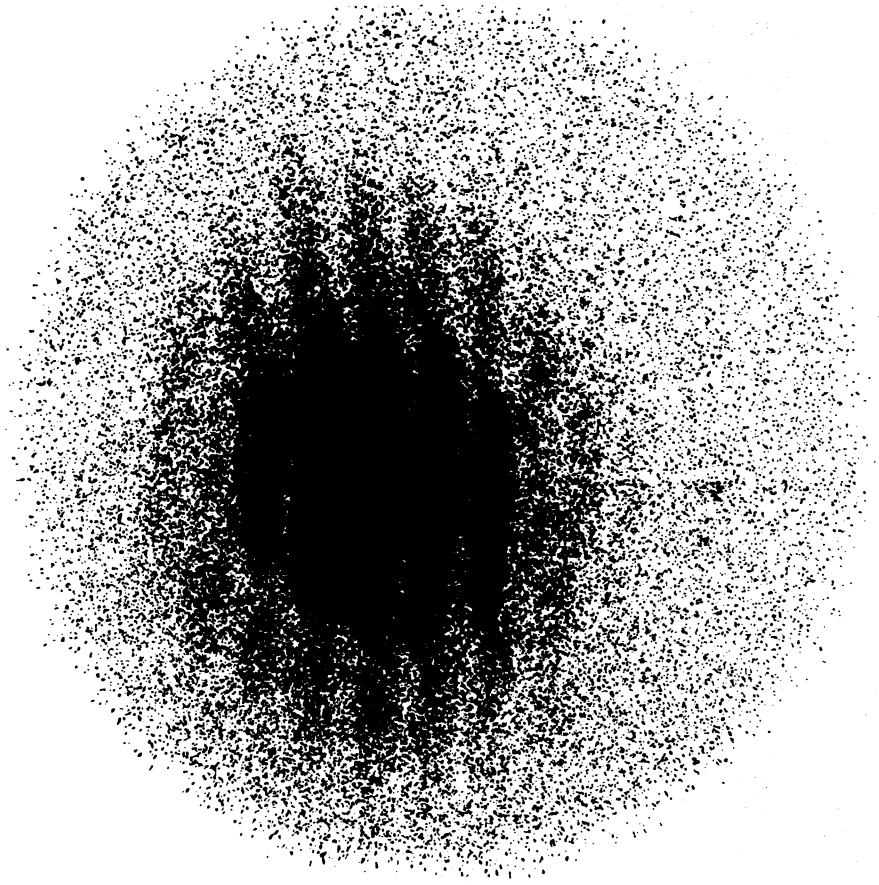

FIGURE 16. Light optical diffractogram of two slightly displaced electron micrographs of the same object. The micrographs are taken under the same electron optical conditions. They are placed one above the other into the diffractometer; so the diffractogram is the square of the sum of the Fourier transform of the two images.

both micrographs into the beam. Therefore the performance of the instrument can be checked quickly. The stripes of the modulation function are easily recognizable in the diffractogram. It has already been noted, that the nodes of the pupil function might be obscured in regions of high spatial frequency. (Due to the borders of the image: the (diffuse) 'image points' at the border of the image will be cut off; see Hoppe (1970*a*).) As the wavelength of this modulation depends only on the displacement, it can be seen also in Fourier regions, where the structure of the pupil function has entirely disappeared. In order to demonstrate the principle, figure 16 shows a light diagram of two exposures of a carbon foil, taken in our older Elmiskop Ia installation. The Fourier region, occupied by these stripes, corresponds to a physical resolution limit of 0.36 nm. Additional calculations have shown, that the chromatic aberration (not the spherical aberration!) is responsible for the limit in this case. (A conventional high tension set was used for this experiment.)

PHILOSOPHICAL TRANSACTIONS OF THE ROYAL SOCIETY B BIOLOGICAL SCIENCES

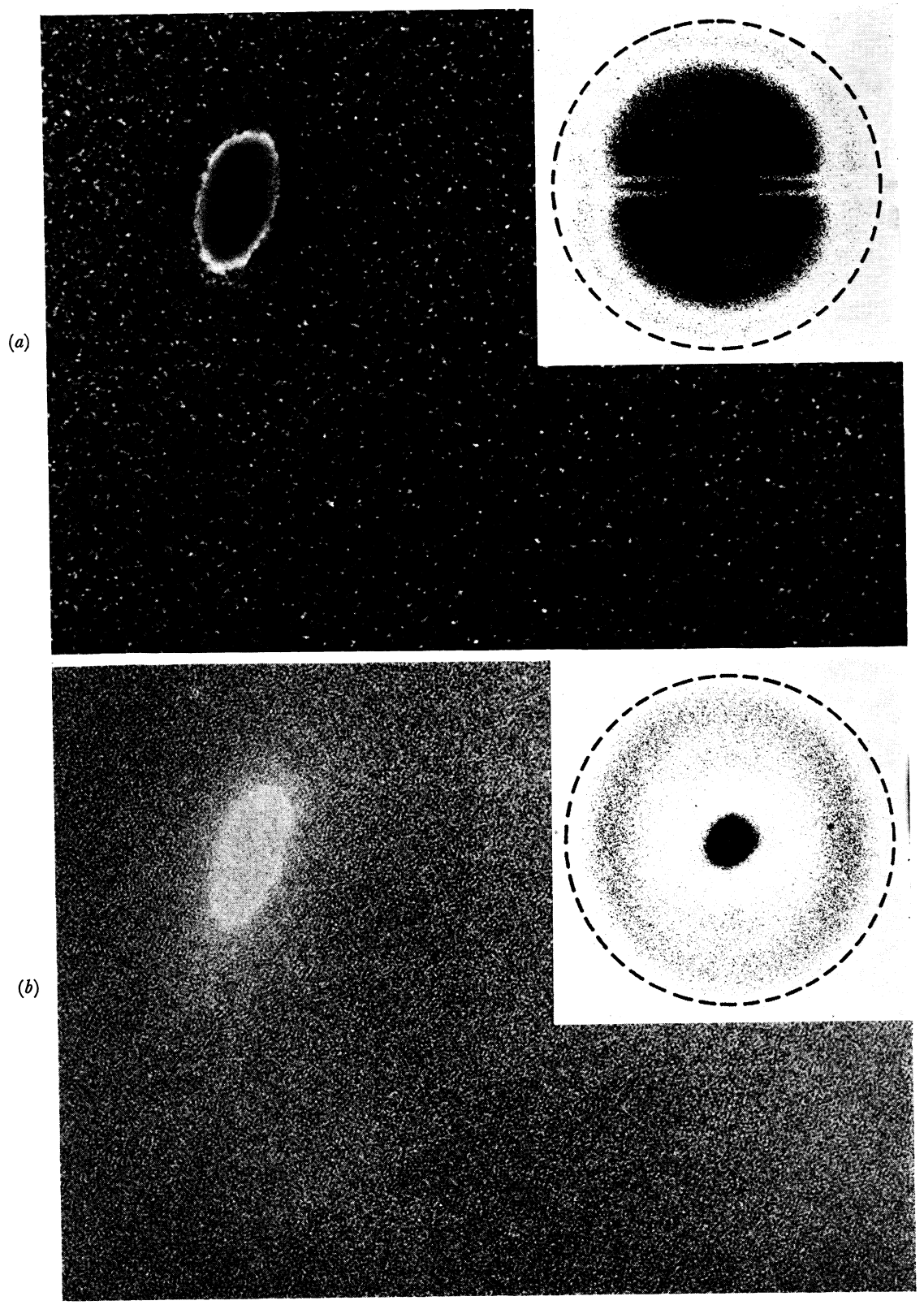

FIGURE 6. Micrographs and corresponding optical transforms of a thin in focus carbon film containing a hole. A phase plate having a 0.4 μm diameter thread and a 30 μm aperture diameter was used in taking (*a*) and a normal 30 μm objective aperture was used in taking (*b*). The scale of the optical transforms is indicated by the broken circles representing the aperture edges (β = 9.4 mrad.). (Magn. × 1 250 000.)

PHILOSOPHICAL TRANSACTIONS OF THE ROYAL SOCIETY B BIOLOGICAL SCIENCES